Screening of modular supramolecular star polymers for 3D printing of biomedical devices

Materials Today Communications 45 (2025) 112206

Contents lists available at ScienceDirect

Materials Today Communications

journal homepage: www.elsevier.com/locate/mtcomm

Screening of modular supramolecular star polymers for 3D printing of biomedical devices

Lewis R. Hart [a], Adja B.R. Touré [b], Robert Owen [c,d], Nur R.E. Putri [b], Richard J.M. Hague [b], Morgan R. Alexander [c], Felicity R.A.J. Rose [c,d], Zuoxin Zhou [b], Derek J. Irvine [b], Laura Ruiz-Cantu [b], Lyudmila Turyanska [b], Yinfeng He [b,e], Wayne Hayes [a], Ricky D. Wildman [b,*]

[a] Department of Chemistry, University of Reading, Reading RG6 6AD, UK
[b] Faculty of Engineering, University of Nottingham, Nottingham NG7 2RD, UK
[c] School of Pharmacy, University of Nottingham, Nottingham NG7 2RD, UK
[d] Nottingham Biodiscovery Institute, University of Nottingham, Nottingham NG7 2RD, UK
[e] Nottingham Ningbo China Beacons of Excellence Research and Innovation Institute, University of Nottingham Ningbo China, Ningbo 315100, China

ARTICLE INFO

Keywords:
Modular polymers
Additive manufacturing
Material screening
Cartilage
Regenerative medicine
Biomaterial discovery

ABSTRACT

Identifying suitable materials for additive manufacturing and 3D printing is a challenging task and there is a need to streamline the processes to achieve more rapid adoption of new feedstocks. We have developed a process of using modular supramolecular polymers where individual moieties can be modified in order to achieve a variance in properties. We synthesised a library of 64 polymers and performed a systematic sequence of screening steps to identify preferred candidates for an exemplar printing modality and application. The library was screened for materials amenable to inkjet based 3D printing, then refined to those that had mechanical and biological performance suitable for use in articular cartilage repair, and supported chondrocyte growth. The lead candidate was fabricated into macroscopic architectures with intricate designs, including structure of knee cartilage as a demonstrator of potential application. This strategy for screening materials for specific applications could accelerate the translation of new materials for additive manufacture of novel devices.

1. Introduction

With the emerging acceptance and adoption of additive manufacturing the need for new materials that can be utilised within these technologies is growing [1,2]. Identifying suitable functional materials is a challenging task; not only is it necessary to ensure their functionality, but materials need to processable and these demands are often in opposition to each other [3]. Furthermore, in some areas of application (e.g., aerospace, healthcare) materials must meet regulatory constraints [4–6]. Therefore, selection criteria are multivariate, leading to time consuming iterative approaches to selection and optimisation, or a weakening of constraints resulting in a 'best-compromise' or sub-optimal performance and a significant bottleneck in developing and adopting materials for additive manufacturing [7,8].

Generally, the materials innovation research effort is focused on development of new chemical compounds or reformulation of existing compounds [9,10], and this has yielded promising solutions, but any minor alteration requires repetition of the full material development and characterization cycle. An alternative approach is to create a library of molecules with pre-designed opportunities for chemical variations to fine tune the physical, chemical or biological properties [11,12]. Emergent techniques, such as predictive statistical analysis and machine learning, could then guide the material design *a priori* in line, which were successfully integrated into additive manufacture of metals [13,14]. Identification of materials for biomedical applications is particularly challenging as they need to be biocompatible and processable whilst capable of satisfying the material integrity requirements [15–18]. High throughput screening approach has been employed successfully in other fields, such as rapid chemical synthesis and screening of materials against particular biological functions [19,20], and is beginning to be explored in additive manufacturing [21] [22].

Of particular interest are supramolecular polymer compounds,

* Corresponding author.
E-mail address: ricky.wildman@nottingham.ac.uk (R.D. Wildman).

https://doi.org/10.1016/j.mtcomm.2025.112206
Received 2 September 2024; Received in revised form 28 February 2025; Accepted 11 March 2025
Available online 13 March 2025

which allow a greater diversity in network forming and may offer a facile route to tune the final properties of structures by controlling the self-assembly process during additive manufacture and post-processing through modulation of chemical moieties and solvent evaporation [23]. Among AM technologies, inkjet based additive manufacturing offers advantages for manufacture of polymers due to its inherent scalability for personalised mass manufacture[24–27].

Here, we develop a strategy for the design and screening of supramolecular materials for inkjet based additive manufacturing, that has the potential to overcome the difficulties posed by current iterative approaches to identifying materials for additive manufacturing, and exemplify its potential by targeting cartilage repair applications (Fig. 1). Such an application is pertinent – many materials for cartilage repair have been investigated previously, but either suffer from poor mechanical properties (e.g., naturally derived hydrogels such as collagen) or poor innate bioactivity (e.g., PEG, PCL or PLGA based materials) [28,29]. Being able to target materials that offer matched mechanical and biological performance will open up future avenues for adoption. Our approach began with the development of a supramolecular polymer library (Fig. 1a) where the components of the polymer compounds, i.e. core, linker, oligomer and assembly motif, can be considered modular offering multiple options for assembly. Each of the options provides property variation, enabling opportunities for fine-tuning of mechanical and/or biological performance. A set of polymer compounds identified as suitable for scalable synthesis was screened to downselect for printability, mechanical performance, and compatibility with relevant cell types (Fig. 1b). A representative candidate material was used to demonstrate successful inkjet additive manufacturing of a cartilage patch for articular cartilage repair (Fig. 1c). This strategy for prescreening materials and informed design of polymers with tailored properties could accelerate the translation of new materials for additive manufacture of novel devices, whilst also creating materials properties libraries ready for future mechanistic studies.

2. Materials and methods

2.1. Materials

Starting materials and reagents were purchased from Sigma Aldrich/Merck UK and used as received unless otherwise stated. Synthesis and analysis are reported in the supplementary information.

2.2. Characterisation

^{1}H NMR and ^{13}C NMR spectra were recorded on either a Bruker Nanobay 400 or a Bruker DPX 400 spectrometer operating at 400 MHz for ^{1}H NMR or 100 MHz for ^{13}C NMR spectroscopic analysis. Data were processed using MestReNova Version 11.0.3–18688. Samples for NMR spectroscopic analysis were prepared in $CDCl_3$, d_6 DMSO or d_8-THF, and dissolution of the sample was aided by gentle heating. Chemical shifts (δ) are reported in ppm relative to tetramethylsilane (δ 0.00 ppm) for $CDCl_3$ and the residual solvent resonance (δ 2.50 ppm) for d_6-DMSO and (δ 1.73 ppm) for d_8-THF for ^{1}H NMR spectroscopic analysis.

Infrared (IR) spectroscopic analysis was carried out using a Perkin Elmer 100 FT-IR (Fourier Transform Infrared) instrument with a diamond-ATR sampling accessory.

An Agilent Technologies 1260 Infinity system was used to obtain gel permeation chromatography (GPC) analysis in HPLC-grade THF at a flow rate of 1.0 mL/min. Calibration was achieved using a series of near monodisperse polystyrene standards, and samples were prepared at a concentration of 1 mg/mL.

2.3. Solubility and printability

The first step of the screening process saw each polymer dissolved in DMAC at 200 mg/mL. Any material that formed a gel or precipitate was deemed unfit for inkjet printing and discarded. Viscosity and surface tension were measured using a high throughput screening method previously developed in order to calculate the Z parameter [30] 300 μL of each sample was added into a 96-well polypropylene plate containing 1 mL wells (260252, Thermo Scientific), and maintained at 25 °C prior to determining viscosity and surface tension.

2.4. Microarray fabrication

Microarrays were fabricated using a Biodot XYZ3200 contact printer and super hydrophilic-super hydrophobic slide (Aqua Array GmbH, DMA Slide 2187, 500 μm square 3 fields). Polymer solutions were prepared in N,N-dimethylformamide (DMF) at 200 mg/mL. 20 μL of each formulation was deposited into a unique well of a 384 polypropylene well plate. A ceramic pin of 0.5 mm diameter was used for all pin printing.

2.5. Atomic force microscopy (AFM)

AFM measurements were conducted using a Dimension FastScan Bio AFM (Bruker Nano Surfaces Division, Santa Barbara, CA USA) equipped with a motorised xy stage as previously described [31]. Briefly, measurements were operated with a Nanoscope controller operated in a PeakForce Quantitative NanoMechanics (QNM) mode in air using a silicon tips with a resonant frequency of 150 kHz and a force constant of approximately 6 N/m (RTESPA-150, Bruker Nano Inc., Camarillo, CA

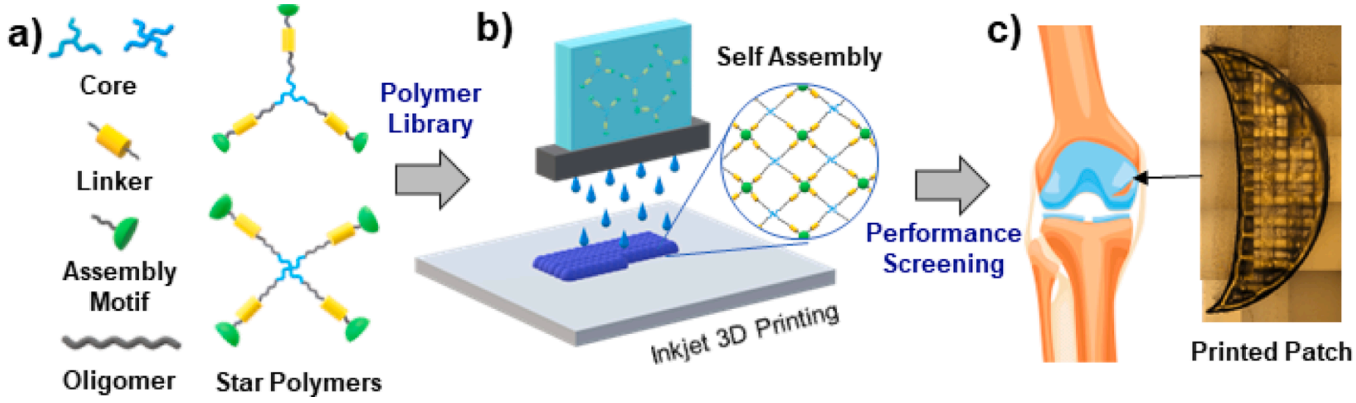

Fig. 1. Schematic diagram of the material screening strategy for identifying a supramolecular material for cartilage repair: a) three-arm and four-arm star polymers comprised of a core, oligomer, linker, and assembly motif were synthesized to create a supramolecular polymer compound library; b) star polymer compounds were developed into ink formulations that can self-assemble after the inkjet based 3D printing process to construct solid structures; c) the screening process allowed us to identify a polymer candidate that is compatible with the inkjet printing process and suitable for cartilage repair.

USA). 5 μm × 5 μm surface area scans were imaged. NanoScope Analysis software (v1.9) was used for data analysis.

2.6. Inkjet printing

Polymer **32** was printed using a Dimatix materials printer (DMP 2830, Fujifilm) with a piezoelectric based jetting system equipped with a disposable 16 nozzle printhead with 10pL droplet size (DMC-11610, Fujifilm). Prior to printing, polymer **32** was dissolved in dimethylacetamide:chloroform at a ratio of 2:1 at 60 °C to create an ink, which was added to the cartridge using a needle and syringe prior to insertion into the Dimatix printer. Printhead temperature was set at 60 °C and polyethylene naphthalene (PEN) maintained at 40 °C was used as a substrate.

Where a sacrificial ink was co-printed to allow channel formation was used, the water soluble ink was prepared by adding 2 wt% 2,4-diethyl-9H-thioxanthen-9-one (98 %) and 2 wt% ethyl 4-(dimethylamino)benzoate (99 wt%) to 4-acryloylmorpholine (97 %), stirring at room temperature (800 rpm) until all additives were fully dissolved, then filtering with a PTFE-based syringe filter prior to use. When using support materials, printed samples were immersed in deionized water for 10 min to fully remove the support.

2.7. Plasma treatment

A tabletop Diener plasma system was used for all plasma treatments. Samples were placed inside the chamber and the pressure reduced to 0.2 mbar. The chamber was flushed 5 times with pure oxygen by cycling between 0.2 and 2.0 mbar before adjusting the pressure to 0.25 mbar to achieve a constant oxygen flow rate through the chamber. Oxygen plasma was generated at this flow rate for two minutes to treat samples.

2.8. Contact angle measurement

The sessile drop technique was used to measure the water contact angle on samples using a Kruss DSA 100 drop shape analyzer at room temperature. Contact angles were determined using the analyzer's software. Two types of samples were prepared from polymer **32**: inkjet printed and cast. The cast sample was made by dropping warm polymer **32** ink onto a heated PEN substrate to create a flat film. Three layers of polymer **32** ink were printed in accordance with §2.6 to form an 8 × 30 mm square. Contact angles were determined for both sample types with and without plasma treatment.

2.9. Biological studies

Biological assessment of suitability for cartilage repair was performed with primary ovine chondrocytes harvested and cultured from the articulating surface of the sheep chondyle as previously described [32]. Sheep condyles were collected from surplus tissue from a study being conducted at the University of Nottingham carried out in accordance with UK Home Office Regulations, and approved by the University of Nottingham Animal Welfare and Ethical Review Body (AWERB). Chondrocytes cells were expanded in chondrocyte growth media (CGM, α-MEM (BioWhittaker Reagents, Lonza Walkerville Inc, United States), 5 % FBS, 2 mM L-Glutamine, 50 μg/mL ascorbic acid 2-phosphate, 50 μg/mL L-proline, 100 mg/mL penicillin-streptomycin, and 0.25 mg/mL amphotericin B. For experiments, CGM was supplemented with 1 × Insulin-Transferrin-Selenium (ITS, ThermoFisher), 10 ng/mL TGF-β1, and 5 ng/mL FGF-2 (Peprotech).

Initial biocompatibility of candidate formulations was assessed via extract cytotoxicity testing in line with ISO 10993–5. Triplicates of casts of each formulation were made by dissolving the polymers in dimethylacetamide in HPLC vials and then evaporating the solvent in a vacuum oven for 5 days. Polymers were washed twice with deionised water, UV sterilised (270 nm) for 20 min, then PBS rinsed before extraction at 0.1 g/mL in culture medium for 72 h at 37 °C to allow leaching of any cytotoxic components. Chondrocytes were seeded at 10,000 cellls per well in a 96 well plate in CGM and allowed to adhere for 24 h at 37 °C, 5 % CO_2 in air before applying 200 μL of extract for a further 24 h. CGM was incubated under the same conditions and was used as a live control. Exposure to 70 % (*v/v*) ethanol for 15 min immediately prior to analysis was used a dead control. Cytotoxicity was assessed by quantifying metabolic activity using PrestoBlue™ (ThermoFisher, UK) in accordance with manufacturer instructions, with a greater than 30 % reduction *versus* the live control classed as toxic. Briefly, media was removed from wells, replaced with PrestoBlue™ diluted 1:10 in CGM, incubated for 1 h at 37 °C 5 % CO_2 in air, then the solution transferred to a black 96-well plate and fluorescence read at λ_{ex}: 560 nm, λ_{em}: 590 nm in a plate reader (Tecan Infinite 200, Switzerland as a correlation with metabolic activity.

To assess the effects of plasma treatment, samples were place in a 24 well plate and seeded at 100,000 cells/cm^2 and maintained for either 24 h or 72 h (as described above) before LIVE/DEAD (ThermoFisher, UK) quantification in accordance with manufacturer instructions. Live and dead controls were cultured on tissue culture plastic with dead cells killed by exposure to 70 % (*v/v*) ethanol for 15 min immediately prior to analysis. To perform the assay, media was replaced with 2 μM calcein AM and 4 μM ethidium homodimer-1 in PBS and incubated for 20 min at 37 °C 5 % CO_2 in air. Staining solution was replaced with PBS before imaging with a fluorescence microscope (Nikon Eclipse Ti). Image analysis was performed using CellProfiler (v2.2.0) by segmenting live (green) and dead (red) cells as primary objects to automate counting of cells (~3000 cells in conditions with the most cells) [9,33].

2.10. Statistical analysis

All data is presented as Mean±SD. Biological data visualisation and analysis was performed using GraphPad Prism and for materials characterisation using R using one-way or two-way analysis of variance (ANOVA) as appropriate with Tukey's post-hoc test. p values < 0.05 were considered significant. Factor analysis of mixed data was performed using R.

3. Results and discussion

3.1. Supramolecular polymer compound library

With the specific aim of generating a new biocompatible polymer suitable for deposition via inkjet printing methods, we started with a library of 64 potential 'modular' supramolecular polymers (**1-64**), each composed of the following components: core (C), oligomer (O), linker (L) and assembly motif (M) (see Fig. 2a, Table S1 in the Supplementary). To provide diversity, one from a range of up to four different moieties were chosen for each component: C: three or four arm stars; O: polycaprolactone of four different molecular weights (5, 10, 15 and 20 kDa); L: four di-isocyanate reactive linkers including both aliphatic and aromatic structures; M: two capping moieties (Fig. 2, Table S1), providing potential for either covalent or associative non-covalent bonding. As a note, two other capping moieties were also assessed: ureidopyrimidone was found to produce crystallinity when coupled to polycaprolactone (PCL) stars, and acrylate which was found to be difficult to purify and after preliminary tests were abandoned and not included in this screening experiment [34]. All of the polymers synthesised were characterised by NMR spectroscopy, and their structural integrity determined (see the SI and Extended Data for details on the synthetic methods used and the analytical data for these polymers).

The 64 materials (**1-64,** Supplementary Table S1) were then formulated into inks screened for parameters that dictate their amenability to inkjet printing (Fig. 2b): (1) ability to form a stable solution when dissolved, (2) ability to form a solid material under standard temperature and pressure (STP) after solvent evaporation, and (3) a *Z* parameter within the range associated with inkjet printability. The *Z*

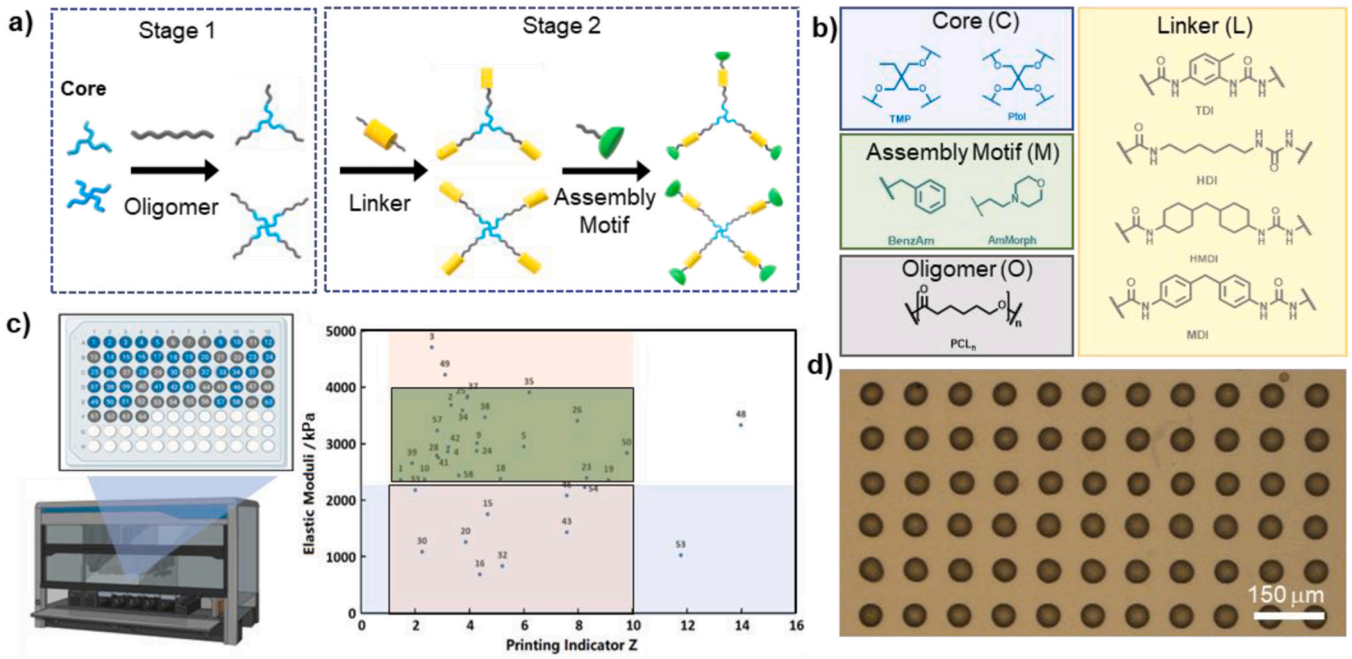

Fig. 2. a) The star polymer compounds were synthesized by stepwise attachment of the selected moieties to the oligomer core; b) A library of 64 star polymers was synthesized from the combination of two cores, four assembly motifs, chain extenders of four lengths, and four linkers; c) A printability screening process revealed 34 suitable candidates, of which 9 had an elastic modulus (green highlighted region) appropriate for cartilage repair and; d) printability of polymer 32.

parameter, an inverse Ohnesorge number ($Z = 1/Oh$), is calculated from the viscosity and surface tension and classifies inks that fall within the range $1 > Z > 10$ as suitable for standard inkjet printheads [21,35].

Of the 64 polymers, 12 were found to either form a precipitate or a gel when dissolution in DMAC was attempted, deeming them unsuitable. A further 16 were discarded due to being unable to form a solid material at STP, rendering them unusable for our downstream applications. Finally, we screened the polymers for printability by determining their Z parameter [21] with 2 polymer compounds found to have a Z value that falls outside of the recommended limit for successful inkjet printing.

It was noted that there were conditions where inks could be printed successfully outside of this range, and that some specialized printheads are more suitable for higher viscosity inks [36,37]. Whilst a further adjustment could have been made to reduce the viscosity by increasing the solvent content; the reduced concentration of the polymer would result in additional print time and longer extraction of the solvent. Therefore, the same DMAC concentration was retained throughout the tests. This screening process assigned 34 supramolecular polymers as suitable candidates to be taken forward for the subsequent screening step: assessment of mechanical and biofunctional properties (Fig. 2c and d)

3.2. Characterization of deposited supramolecular polymer compounds

To establish the range of mechanical properties achievable with our formulations, square shaped samples (500 × 500 µm) of each polymer compound were printed as an array onto superhydrophobic-superhydrophilic imprinted microslides. Atomic force microscopy (AFM) revealed that the generated library of materials have elastic moduli in the range of 0.8 MPa to 5 MPa.

To demonstrate applicability of this process to guide the selection of new materials for specific additive manufacturing applications, we chose an exemplar application of cartilage repair. Native articular cartilage has an elastic modulus of approximately 1 MPa, although significant variability is observed [15–18]. Therefore, 10 candidates with the elastic modulus below 2.2 MPa were selected, of which 9 candidates had Z parameter suitable for inkjet printing, and were advanced to biological screening (Green highlighted region, Fig. 2c).

An extract test consistent with ISO 10993–5 that identifies non-cytotoxic materials revealed six polymers on which cells exhibited metabolic activities above 70 % of the live control, classifying them as non-cytotoxic (**15**, **20**, **30**, **32**, **46**, **54**). Cells on four polymers (**16**, **33**, **43**, **54**) showed a metabolic activity significantly below 100 % of the live control. The four leading candidates (**15**, **20**, **32**, **46**) were taken forward for subsequent screening experiments (Fig. 3a).

3.3. Printing trial and fabrication of cartilage replacement structure

To demonstrate the feasibility of using the four leading biocompatible supramolecular polymers for 3D printing of cartilage support structures (**15**, **20**, **32**, **46**) (Table 1), we examined their uniform film forming ability and cell attachment. Films were generated by depositing a drop of each ink formulation onto a glass slide and observing with optical microscopy. Significant coffee ring effects and crack formation was observed for two of the samples (**15**, **20**), while **46** formed a rough and uneven film with minor cracks observed after drying. Only **32** (TMP (C)-PCL5(O)-HDI(L)-Benz-AM(M)) formed a macroscopically uniform film and supported cell attachment (Fig. 3b), and therefore was the selected candidate material for subsequent experiments.

The candidate material **32** was successfully inkjet printed into complex geometries with good fidelity (Fig. 2d) and as scaffold-like mesh structure with 162 µm strut size and 362 µm square voids with a deviation of *ca.* 10 % from the original design (Fig. 4a). A University logo design over 5.5 mm × 7.5 mm (Fig. 4b) and a structure replicating features of a cartilage patch (10 mm wide, Fig. 4c) were printed demonstrating reliable manufacture over larger areas. The moon-shaped patch designed with two tiers of internal channels to increase the surface area, was co-printed using candidate **32** with a UV curable and water-soluble sacrificial material to allow overhanging features (Fig. 4c).

3.4. Performance optimisation of printed samples

Initially, it was found that cell adhesion was poor and insufficient to allow proliferation of chondrocytes and coverage of the inkjet printed

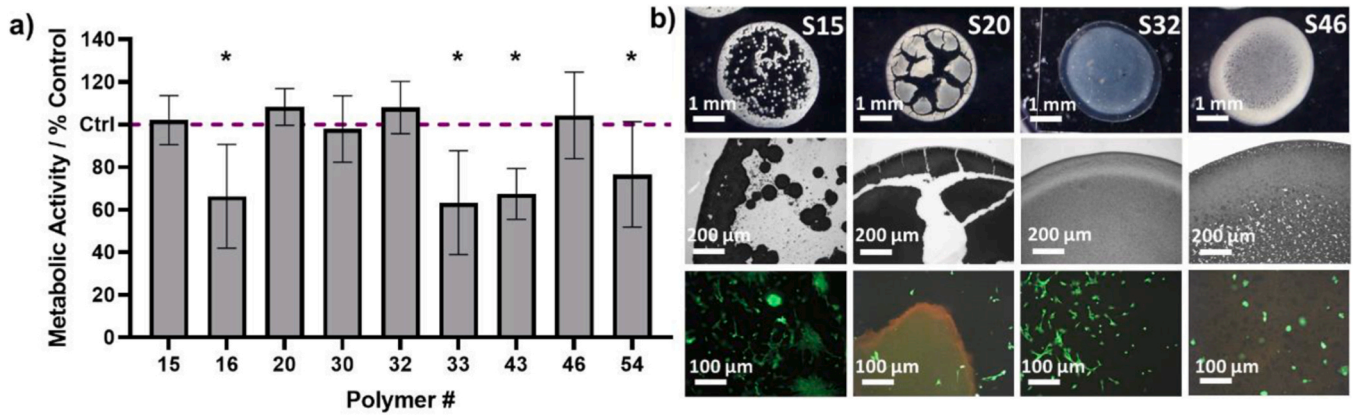

Fig. 3. Screening step to identify biocompatible polymers from available candidates: a) 24 h extract cytotoxicity testing from the 9 candidate materials was performed on chondrocytes (mean±SD, n = 9). Cells cultured in extracts from polymer candidates 16, 33, 43 and 54 showed metabolic activities significantly below the live control, whilst 15, 20, 30, 32 and 46 showed no significant difference in metabolic activity versus the live control (purple dashed line). b) of the four leading candidates, only 32 was able to form a uniform film of material, with all others showing defects under optical microscopy. Chondrocytes showed normal cellular morphology and viability (green; LIVE/DEAD™ staining) 24 h after seeding on 32 when assessed by fluorescence microscopy.

Table 1
Composition of the supramolecular compounds used for cartilage structures.

No.	CORE (C)	Oligomer (O)	Linker (L)	Assembly Motif (M)
15	TMP	PCL15	HMDI	Benz-Am
20	TMP	PCL10	HDI	Am-Morph
32	TMP	PCL5	HDI	Benz-Am
46	Ptol	PCL15	TDI	Benz-Am

structure, with cells preferring to form agglomerates with themselves rather than spreading over the surface. To address this, we subjected both the cast and inkjet printed structures to oxygen plasma treatment, reducing the water contact angle (Fig. 5a and b) and facilitating greater cell adhesion and proliferation (Fig. 5c), as confirmed by LIVE/DEAD™ staining assay. In line with other studies where plasma-treatment has been used to improve cell attachment to hydrophobic materials [38,39], plasma treated samples had significantly more live chondrocytes and a lower percentage of dead cells than their non-treated counterparts at both 24 h and 72 h after seeding (Fig. 5d). With the observation that plasma treatment resulted in a significant reduction in contact angle, we propose that the increased viability of cells was likely due to the enhanced wettability permitting superior protein adsorption and thus cell adhesion and normal cell spreading [40].

A statistical analysis was performed to assess the relationship between compound composition and performance. A linear model with Tukey post-hoc test was constructed to test the relationship between supramolecular polymer composition and modulus, printability and biocompatibility, using four variables (C, O, L, M) associated with each of the modular components of our polymer compounds, with levels representing variation within each of those categories. This indicated that the only statistical significance that could ascribed was between end group and modulus (with AM-Morph resulting in a higher modulus than Benz-AM). A further analysis was then conducted to elucidate any underlying trends not easily identifiable. This used factorial analysis of mixed data to undertake an analysis similar to principal component analysis. The results of this analysis suggested three main trends that could potentially be significant: 1) the length of the PCL based oligomer; 2) the details of the linker, e.g., linear or aromatic, could be influential; and 3) three or four arm polymer compounds may result in different properties. Although more detailed work examining the assembly

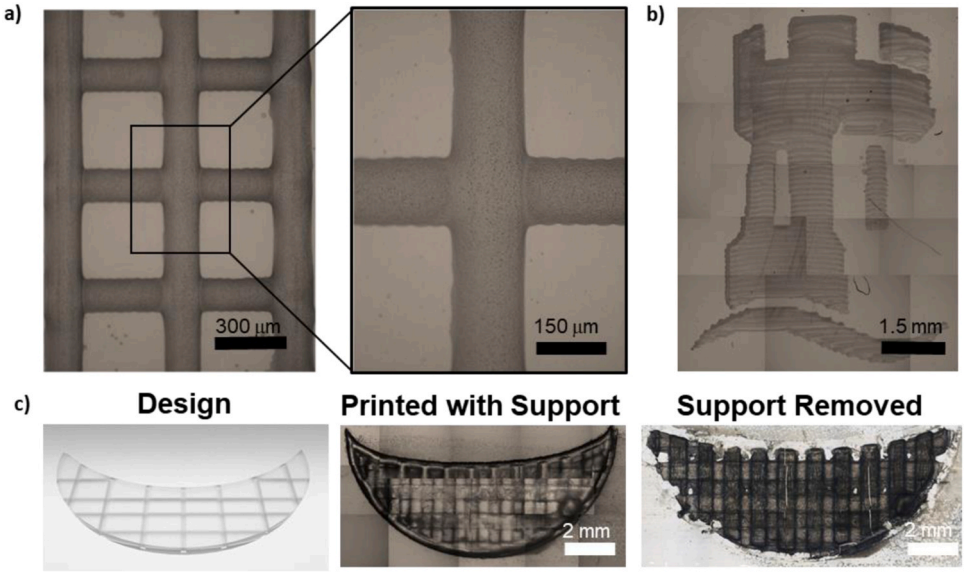

Fig. 4. Structures fabricated via inkjet based 3D printing from the lead candidate material, polymer 32: a) square mesh structure; b) inkjet printed castle logo of University of Nottingham; c) cartilage patch scaffold containing through channels achieved by co-printing with water soluble support materials.

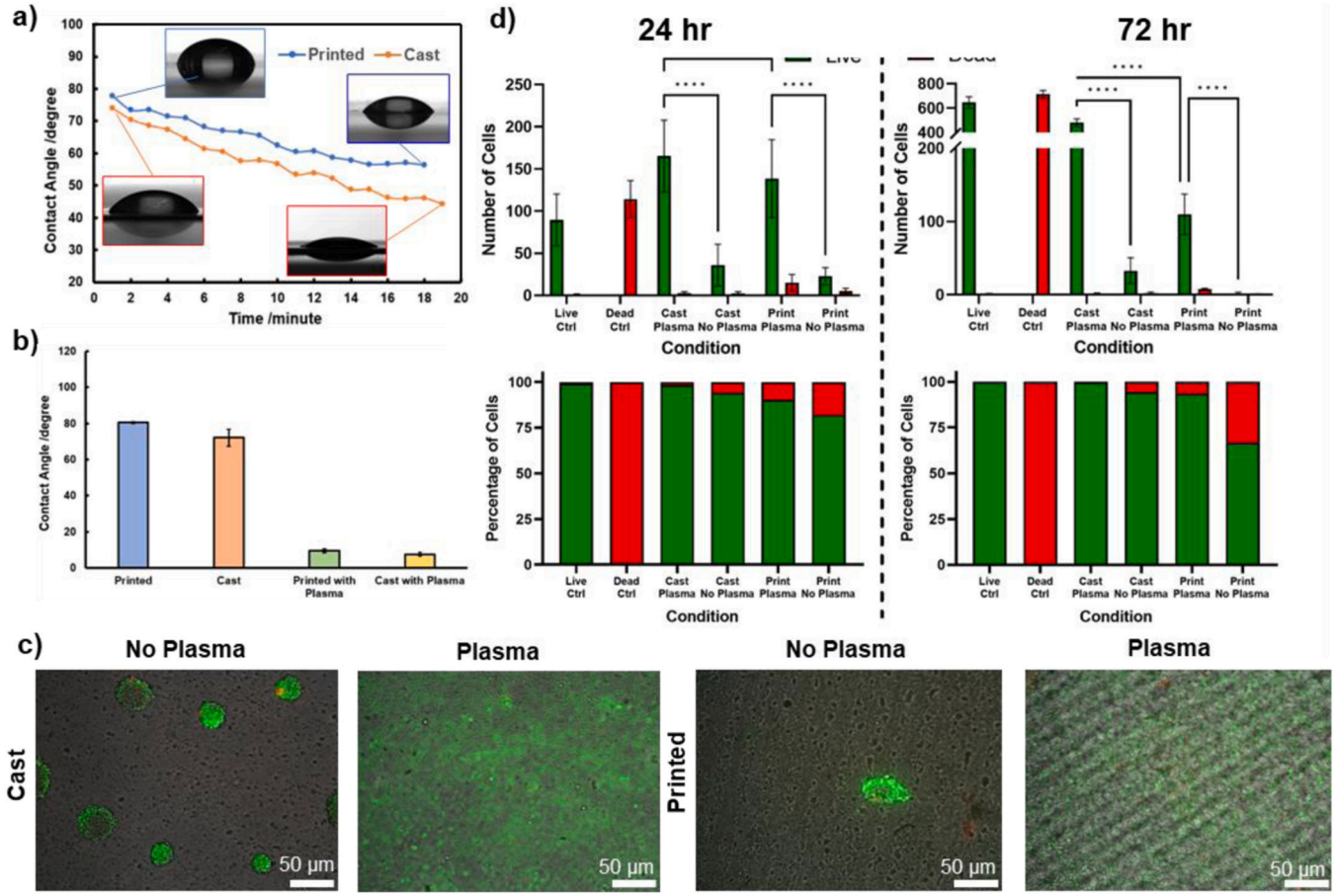

Fig. 5. Performance of 32 following plasma treatment: a) both cast and inkjet printed samples showed high contact angle with deionized water; b) oxygen plasma treatment for 2 min introduces hydrophiliticy to both cast and printed samples and reduced the deionized water contact angle from 80° to 20°; c) chondrocytes were cultured on both cast and printed polymer 32 with and without plasma oxygen treatment. Without plasma, chondrocytes formed agglomerates rather than adhering to the surface. Scale bar 50 µm; d) results of LIVE/DEAD™ assay performed at 24 h (left) and 72 h (right) after seeding showed plasma treated samples supported significantly more live chondrocytes than non-treated at both time points with a lower percentage of dead cells (results are shown as mean±SD of up to ~3000 cells analysed).

behaviour and its effect on e.g., microstructure is required [41–43], we draw the following indicators from our analysis. First, since the morpholine end group can hydrogen bond (unlike the benzyl unit), this likely reinforces the material and creates differences in modulus. Second, the length of the oligomer and the choice of linear or aromatic linkers will likely influence the self-assembly though hydrogen bonding and phase separation, e.g., the longer PCL chains will be more flexible, and there will be a lower entropic cost associated with assembly of networks with more rigid linkers, such as TDI. Finally, the number of arms will have an influence on self assembly through the available end groups, and the number and accessibility of available hydrogen bonding sites [44]. However, the assembly relationships are likely to be non-linear and not easily understood in terms of their link with properties of interest for our application – the link between microstructure and cellular response is not trivial to unpick, and a more sophisticated approach may be needed to determine precise mechanisms in the future.

4. Conclusions

We have demonstrated that it is possible to use a modular approach to identify lead candidates for additively manufactured biomedical devices. A library of supramolecular polymer compounds was synthesised, and using a screening approach, we were able to identify an inkjet-printable compound as a suitable candidate for supporting chondrocyte growth. Using this candidate we were able to undertake further optimisations and demonstrate its usefulness as a material for additive manufacturing, recreating an articular cartilage repair support structure. This modular approach gives a rapid way of producing diverse materials libraries, and can be used for other target devices, potentially employing the same library and assessing materials discarded in this paper for other applications.

CRediT authorship contribution statement

Ruiz-Cantu Laura: Supervision, Methodology, Data curation. **Turyanska Lyudmila:** Writing – review & editing, Writing – original draft, Methodology, Data curation, Conceptualization. **Alexander Morgan R:** Supervision, Funding acquisition, Conceptualization. **Rose Felicity R A J:** Supervision, Funding acquisition, Conceptualization. **Zhou Zuoxin:** Investigation. **Irvine Derek J:** Funding acquisition, Conceptualization. **Touré Adja B R:** Methodology, Investigation, Formal analysis, Data curation. **Hayes Wayne:** Writing – review & editing, Writing – original draft, Supervision, Project administration, Methodology, Funding acquisition, Conceptualization. **Owen Robert:** Writing – review & editing, Writing – original draft, Visualization, Validation, Methodology, Investigation, Funding acquisition, Formal analysis, Data curation. **Putri Nur R E:** Investigation. **Hague Richard J M:** Supervision, Funding acquisition, Conceptualization. **Wildman Ricky D.:** Writing – review & editing, Writing – original draft, Validation, Supervision, Project administration, Methodology, Funding acquisition, Formal analysis, Data curation, Conceptualization. **Hart Lewis R:** Methodology, Investigation, Formal analysis, Data curation. **He Yinfeng:** Writing – review

& editing, Writing – original draft, Visualization, Validation, Supervision, Project administration, Methodology, Formal analysis, Data curation, Conceptualization.

Declaration of Competing Interest

The authors declare that they have no known competing financial interests or personal relationships that could have appeared to influence the work reported in this paper.

Acknowledgements

This work was funded by the Engineering and Physical Sciences Research Council [grant numbers EP/W017032/1 and EP/N024818/1]. RO would like to thank the University of Nottingham for his Nottingham Research Fellowship. The authors wish to acknowledge Dr Jane McLaren, School of Pharmacy, University of Nottingham for the supply of the sheep chondyles used in this study.

Appendix A. Supporting information

Supplementary data associated with this article can be found in the online version at doi:10.1016/j.mtcomm.2025.112206.

Data availability

Data will be made available on request.

References

[1] G. Chyr, J.M. DeSimone, Review of high-performance sustainable polymers in additive manufacturing, Green. Chem. 25 (2) (2023) 453–466.
[2] L.J. Tan, W. Zhu, K. Zhou, Recent progress on polymer materials for additive manufacturing, Adv. Funct. Mater. 30 (43) (2020) 2003062.
[3] M. Ziaee, N.B. Crane, Binder jetting: a review of process, materials, and methods, Addit. Manuf. 28 (2019) 781–801.
[4] I. Gouzman, et al., Advances in polyimide-based materials for space applications, Adv. Mater. 31 (18) (2019) 1807738.
[5] Y. He, M.I.E. Barreiros, H. Cader, Personalized Medicine: Manufacturing Oral Solid Dosage Forms Through Additive Manufacturing, in: K. Zhou (Ed.), in *Additive Manufacturing: Materials, Functionalities and Applications*, Springer International Publishing, Cham, 2023, pp. 113–150.
[6] K. Vithani, et al., An overview of 3D printing technologies for soft materials and potential opportunities for lipid-based drug delivery systems, Pharm. Res. 36 (1) (2018) 4.
[7] S.A.M. Tofail, et al., Additive manufacturing: scientific and technological challenges, market uptake and opportunities, Mater. Today 21 (1) (2018) 22–37.
[8] U.Ku Zaman, et al., Integrated product-process design: material and manufacturing process selection for additive manufacturing using multi-criteria decision making, Robot. Comput. Integr. Manuf. 51 (2018) 169–180.
[9] E. Krumins, et al., Glycerol-based sustainably sourced resin for volumetric printing, Green. Chem. 26 (3) (2024) 1345–1355.
[10] Y. He, et al., Ink-jet 3D printing as a strategy for developing bespoke non-eluting biofilm resistant medical devices, Biomaterials 281 (2022) 121350.
[11] B. Burger, et al., A mobile robotic chemist, Nature 583 (7815) (2020) 237–241.
[12] P.M. Maffettone, et al., Crystallography companion agent for high-throughput materials discovery, Nat. Comput. Sci. 1 (4) (2021) 290–297.
[13] N.S. Johnson, et al., Invited review: machine learning for materials developments in metals additive manufacturing, Addit. Manuf. 36 (2020) 101641.
[14] H.-r Zhou, et al., Advancements in machine learning for material design and process optimization in the field of additive manufacturing, China Foundry (2024).
[15] C.J. Little, N.K. Bawolin, X. Chen, Mechanical properties of natural cartilage and tissue-engineered constructs, Tissue Eng. Part B Rev. 17 (4) (2011) 213–227.
[16] K.M. Arnold, et al., Atomic force microscopy micro-indentation methods for determining the elastic modulus of murine articular cartilage, Sensors 23 (4) (2023).
[17] J. Liu, et al., Hydrogels for engineering of perfusable vascular networks, Int. J. Mol. Sci. 16 (7) (2015) 15997–16016.
[18] R. Olivares-Navarrete, et al., Substrate stiffness controls osteoblastic and chondrocytic differentiation of mesenchymal stem cells without exogenous stimuli, PLOS ONE 12 (1) (2017) e0170312.
[19] L. Yang, et al., High-throughput methods in the discovery and study of biomaterials and materiobiology, Chem. Rev. 121 (8) (2021) 4561–4677.
[20] R. Owen, et al., Computer vision for substrate detection in high-throughput biomaterial screens using bright-field microscopy, Adv. Intell. Syst. (2024) 2400573 (n/a(n/a): p).
[21] Z. Zhou, et al., High-throughput characterization of fluid properties to predict droplet ejection for three-dimensional inkjet printing formulations, Addit. Manuf. 29 (2019) 100792.
[22] M. Vassey, et al., Innate immune cell instruction using micron-scale 3D objects of varied architecture and polymer chemistry: the chemoarchichip, Matter 6 (3) (2023) 887–906.
[23] A.D. O'Donnell, et al., Applications of supramolecular polymer networks, React. Funct. Polym. 172 (2022) 105209.
[24] V.M. Vaz, L. Kumar, 3D printing as a promising tool in personalized medicine, AAPS PharmSciTech 22 (1) (2021) 49.
[25] X. Du, et al., A review of inkjet printing technology for personalized-healthcare wearable devices, J. Mater. Chem. C. 10 (38) (2022) 14091–14115.
[26] G. Rivers, et al., Enabling high-fidelity personalised pharmaceutical tablets through multimaterial inkjet 3D printing with a water-soluble excipient, Mater. Today Adv. 22 (2024) 100493.
[27] J. Ding, et al., The economics of additive manufacturing: towards a general cost model including process failure, Int. J. Prod. Econ. 237 (2021) 108087.
[28] X. Zhao, et al., Applications of biocompatible scaffold materials in stem cell-based cartilage tissue engineering, Front. Bioeng. Biotechnol. 9 (2021).
[29] K.D. Ngadimin, et al., Biomimetic hydrogels designed for cartilage tissue engineering, Biomater. Sci. 9 (12) (2021) 4246–4259.
[30] L. Ruiz-Cantu, et al., Bespoke 3D-printed polydrug implants created via microstructural control of oligomers, ACS Appl. Mater. Interfaces 13 (33) (2021) 38969–38978.
[31] I. Louzao, et al., Identification of novel "Inks" for 3D printing using high-throughput screening: bioresorbable photocurable polymers for controlled drug delivery, ACS Appl. Mater. Interfaces 10 (8) (2018) 6841–6848.
[32] L. Ruiz-Cantu, et al., Multi-material 3D bioprinting of porous constructs for cartilage regeneration, Mater. Sci. Eng. C. Mater. Biol. Appl. 109 (2020) 110578.
[33] D.R. Stirling, et al., CellProfiler 4: improvements in speed, utility and usability, BMC Bioinforma. 22 (1) (2021) 433.
[34] R.P. Sijbesma, et al., Reversible polymers formed from self-complementary monomers using quadruple hydrogen bonding, Science 278 (5343) (1997) 1601–1604.
[35] J.E. Fromm, Numerical calculation of the fluid dynamics of drop-on-demand jets, IBM J. Res. Dev. 28 (3) (1984) 322–333.
[36] B. Derby, Inkjet printing of functional and structural materials: fluid property requirements, feature stability, and resolution, Annu. Rev. Mater. Res. 40 (1) (2010) 395–414.
[37] R. Bernasconi, et al., Piezoelectric drop-on-demand inkjet printing of high-viscosity inks, Adv. Eng. Mater. 24 (1) (2022) 2100733.
[38] R. Owen, et al., Combined porogen leaching and emulsion templating to produce bone tissue engineering scaffolds, Int. J. Bioprint 6 (2) (2020) 265.
[39] R. Owen, et al., Emulsion templated scaffolds with tunable mechanical properties for bone tissue engineering, J. Mech. Behav. Biomed. Mater. 54 (2016) 159–172.
[40] T. Jacobs, et al., Plasma surface modification of biomedical polymers: influence on cell-material interaction, Plasma Chem. Plasma Process. 32 (5) (2012) 1039–1073.
[41] D. Hermida-Merino, et al., The effect of chiral end groups on the assembly of supramolecular polyurethanes, Polym. Chem. 12 (31) (2021) 4488–4500.
[42] D.H. Merino, et al., Thermo-responsive microphase separated supramolecular polyurethanes, Polym. Chem. 1 (8) (2010) 1263–1271.
[43] P.J. Woodward, et al., Hydrogen bonded supramolecular elastomers: correlating hydrogen bonding strength with morphology and rheology, Macromolecules 43 (5) (2010) 2512–2517.
[44] L.R. Hart, et al., Multivalency in healable supramolecular polymers: the effect of supramolecular cross-link density on the mechanical properties and healing of non-covalent polymer networks, Polym. Chem. 5 (11) (2014) 3680–3688.